Published OnlineFirst September 21, 2010; DOI: 10.1158/1535-7163.MCT-10-0265
Published OnlineFirst on September 21, 2010 as 10.1158/1535-7163.MCT-10-0265

Molecular Cancer Therapeutics

Monitoring Molecular-Specific Pharmacodynamics of Rapamycin *In vivo* with Inducible *Gal4→Fluc* Transgenic Reporter Mice

Mei-Hsiu Pan, Jeffrey Lin, Julie L. Prior, and David Piwnica-Worms

Abstract

Rapamycin (Rap), a small-molecule inhibitor of mTOR, is an immunosuppressant, and several Rap analogues are cancer chemotherapeutics. Further pharmacologic development will be significantly facilitated if *in vivo* reporter models are available to enable monitoring of molecular-specific pharmacodynamic actions of Rap and its analogues. Herein we present the use of a *Gal4→Fluc* reporter mouse for the study of Rap-induced mTOR/FKBP12 protein-protein interactions *in vivo* with the use of a mouse two-hybrid transactivation strategy, a derivative of the yeast two-hybrid system applied to live mice. Upon treatment with Rap, a bipartite transactivator was reconstituted, and transcription of a genomic firefly luciferase reporter was activated in a concentration-dependent (K_d = 2.3 nmol/L) and FK506-competitive (K_i = 17.1 nmol/L) manner *in cellulo*, as well as in a temporal and specific manner *in vivo*. In particular, after a single dose of Rap (4.5 mg/kg, i.p.), peak Rap-induced protein-protein interactions were observed in the liver at 24 hours post treatment, with photon flux signals 600-fold over baseline, which correlated temporally with suppression of p70S6 kinase activity, a downstream effector of mTOR. The *Gal4→Fluc* reporter mouse provides an intact physiologic system to interrogate protein-protein interactions and molecular-specific pharmacodynamics during drug discovery and lead characterization. Imaging protein interactions and functional proteomics in whole animals *in vivo* may serve as a basic tool for screening and mechanism-based analysis of small molecules targeting specific protein-protein interactions in human diseases. *Mol Cancer Ther; 9(10); OF1–9. ©2010 AACR.*

Introduction

The mammalian target of rapamycin (mTOR) is a 289-kDa serine-threonine kinase important in regulation of cell growth and proliferation (1, 2). Functions of mTOR can be inhibited by the small-molecule rapamycin (Rap) through formation of a ternary complex comprising Rap, FKBP12 (the 12-kDa immunophilin family member FK506-binding and Rap-binding protein), and mTOR through its FKBP-rapamycin–binding (FRB) domain (3).

Rap is a Food and Drug Administration–approved immunosuppressant agent used to prevent organ rejection after transplantation (4). In addition, Rap and Rap analogues, alone or in combination with other drugs, are undergoing clinical trials for treatment of metastatic and advanced cancers, including brain, breast, and other solid tumors (5, 6). Recently, a Rap analogue, temsirolimus, has been approved for use in treating advanced renal cell carcinoma (7). Mechanistically, Rap provides temporal and quantitative control of gene expression through its ability to associate with FKBP12 and FRB, which are critical in the mTOR signaling pathway through regulating protein translation and controlling autophagy (8, 9). Given that many questions about mTOR complex signaling remain unanswered, gaining insight into the pharmacologic action of Rap and analogues at the molecular level *in vivo* may address many of these questions (10).

Pharmacodynamic analysis is key during early-phase clinical trials to determine the relationships between drug dose and target inhibition, as well as to monitor downstream effects of target inhibition (11). Most conventional methods to monitor pharmacodynamics, including Western blot analysis, immunohistochemical staining, or flow cytometry determinations, require either labor-intensive sample preparation procedures or high-quality monoclonal antibodies and cannot readily provide information about drug effects over time or in intact organ systems (11–13). Integration of genome-wide analysis, proteomics, and bioinformatics can assist the development of pharmacodynamic or pharmacokinetic evaluation by a systematic approach (14–16), but these techniques are at a relatively early stage of development.

Authors' Affiliation: Molecular Imaging Center, Mallinckrodt Institute of Radiology, BRIGHT Institute, and Department of Developmental Biology, Washington University School of Medicine, St. Louis, Missouri

Note: Supplementary material for this article is available at Molecular Cancer Therapeutics Online (http://mct.aacrjournals.org/).

Corresponding Author: David Piwnica-Worms, Mallinckrodt Institute of Radiology, Washington University School of Medicine, 510 South Kingshighway Boulevard, Box 8225, St. Louis, MO 63110. Phone: 314-362-9359; Fax: 314-362-0152. E-mail: piwnica-wormsd@mir.wustl.edu

doi: 10.1158/1535-7163.MCT-10-0265

Published OnlineFirst September 21, 2010; DOI: 10.1158/1535-7163.MCT-10-0265

Recent advances in molecular imaging combined with reporter animals can recapitulate genomic alterations in human diseases and are reshaping the process of new drug development at many levels (17). First, an effective readout reflecting real-time pharmacodynamic changes can be a powerful tool to monitor therapeutic effects in a spatially specific and tissue-specific manner. Second, molecular imaging may reduce cost during drug development because pharmacodynamic studies in animals can inform clinical trials and accelerate the translation process (18, 19). Third, noninvasive imaging allows chronological monitoring for delayed activities and toxicity of drugs in living animals. However, one of the major challenges in *in vivo* pharmacodynamic monitoring is the lack of high-fidelity reporter models to visualize the pharmacodynamics of therapeutic agents in a mechanistically appropriate manner. In this regard, with the use of a universal *Gal4→Fluc* reporter mouse (20), the inducible association of FRB and FKBP12 upon introduction of Rap enabled conditional activation of a luciferase reporter gene (Fig. 1; refs. 21–25). This platform could lead to broader applications of reporter models to study pharmacodynamics in the context of whole animals.

Materials and Methods

Chemicals and reagents

Plasmids *pBJ5-Frb-VP16-HA* and *pBJ5-Gal4-FKBP(X3)*, which express FRB-VP16-HA and G4BD-FKBP(X3) chimera proteins from a modified SV40 (SRα) promoter, were graciously provided by Dr. Thomas Wandless and Dr. Gerald Crabtree (Department of Chemical and Systems Biology, Stanford University, Palo Alto, CA; ref. 26). *pRluc-N3* was purchased from BioSignal Packard. D-Luciferin was obtained from Biosynth, and both rapamycin and FK506 were from Sigma-Aldrich. Native coelenterazine was from Biotium.

Cell cultures and transfection

HeLa/*Gal4→Fluc* cells, HeLa cells that stably express firefly luciferase under the control of a concatenated *Gal4* promoter (5× *Gal4*), were described previously (20). HeLa/*Gal4→Fluc* cells were maintained in DMEM containing 10% heat-inactive fetal bovine serum and 1% glutamine. Transfections were done with FuGENE-6 (Roche) according to the manufacturer's protocol.

Construction of *Frb* mutant plasmid, *mtFrb* (S2035I)

Mutant *Frb* (S2035I), hereafter referred to as *mtFrb*, was prepared by the QuikChange mutagenesis method (Stratagene) according to the protocol provided by the manufacturer. Briefly, PCR was done with the parent plasmid *pBJ5-Frb-VP16-HA* and overlapping oligonucleotides containing relevant base changes (sense primer: 5′-gcatgaaggcctggaagaggcaattcgtttgtactttgg-3′; antisense primer: 5′-ccaaagtacaaacgaattgcctcttccaggccttcatgc-3′). The product was religated to the parent vector and then transformed into TOP10-competent *Escherichia coli* (Invitrogen). The expected mutation was confirmed by sequencing.

Bioluminescence imaging of cells

HeLa/*Gal4→Fluc* cells (2.5×10^5 cells per well for 24-well plates; 1×10^5 cells per well for 96-well plates) were transiently cotransfected with pairs of plasmids (200 ng DNA each for 24-well plates; 30 ng each for 96-well

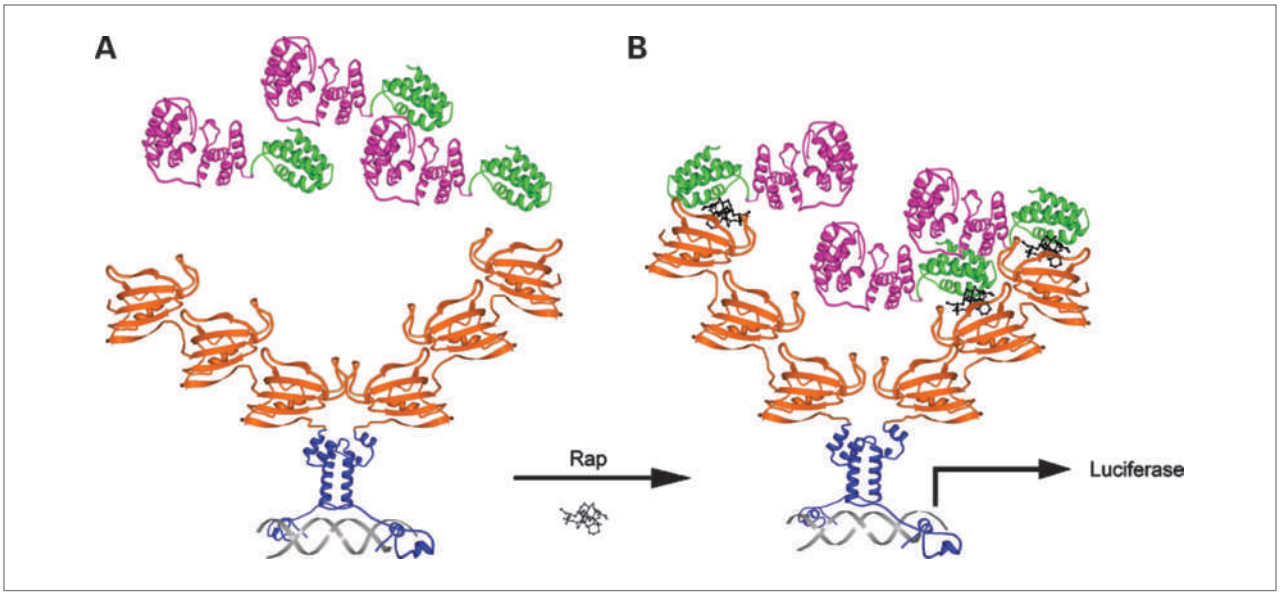

Figure 1. Conditional genomic reporter activation with the use of a modified two-hybrid system. A, a crystallographic model of FRB-VP16 and G4BD-FKBP(X3) domains in the absence of Rap. B, Rap-induced association of FRB-VP16 and G4BD-FKBP(X3) activate the reporter gene, *Fluc* (FRB-VP16, green-magenta; G4BD-FKBP(X3), blue-orange; Rap, black; DNA, gray). Images adapted from RCSB PDB (www.pdb.org) using ID# 1AUE, 2PHG, 3COQ, and 1FKL.

plates) with the use of FuGENE-6 according to the manufacturer's directions. For bioluminescence imaging, ~48 hours after transfection, growth media were replaced with optically clear DMEM containing appropriate drugs or vehicle, and D-luciferin (150 μg/mL; ref. 27). Cells were incubated for another 6 hours, and photon flux for each well was then measured with a charge-coupled device camera (IVIS 100, Caliper) with the use of the following parameters: exposure, 3 minutes; f-stop, 1; binning, 8; field of view, 15 cm; filter, open. Experiments were done in triplicate. After IVIS imaging, an MTS assay for viable cell mass was done according to the manufacturer's instructions (Promega). MTS reagent (20 μL) was added to each well of a 96-well plate at a final volume of 200 μL per well. Samples were incubated for ~1 hour. Absorbance of samples was measured against a background control (blank) at 490 nm. Data normalized by cell mass were expressed as mean photon flux ± SE of triplicate wells (representative of three independent experiments).

Rap concentration-response curve and FK506 competitive inhibition assay

To determine the apparent K_d of Rap-induced FRB and FKBP12 association, as well as the apparent K_i of FK506-mediated inhibition of protein association in live cells, HeLa/*Gal4→Fluc* reporter cells transfected with *pBJ5-Frb-VP16-HA* and *pBJ5-Gal4-FKBP(X3)* plasmid pairs were pretreated with Rap alone for 6 hours before bioluminescence imaging with the indicated concentrations (0.1, 0.3, 1, 3, 10, 30, 100, and 1,000 nmol/L) or with Rap at the EC_{50} (1 nmol/L) in the presence of the indicated concentrations of FK506 (1, 3, 10, 30, 100, and 1,000 nmol/L).

Animal studies

Hydrodynamic injections. Animal care and protocols were approved by the Washington University Medical School Animal Studies Committee. Generation of the *Gal4→Fluc* transgenic reporter mouse strain was described (20). *In vivo* hepatocyte transfection of *Gal4→Fluc* reporter mice was done with the use of the hydrodynamic somatic gene transfer method, as described previously (20). Briefly, plasmid pairs of *pBJ5-Frb-VP16-HA* and *pBJ5-Gal4-FKBP(X3)*, or *pBJ5-mtFrb-VP16-HA* and *pBJ5-Gal4-FKBP(X3)* (15 μg per plasmid), together with *pRluc-N3* (1 μg) were co-injected as indicated. Plasmids were diluted in calcium- and magnesium-free PBS (pH 7.4; 1 mL/10 g of body weight) and rapidly injected into tail veins of mice.

In vivo *bioluminescence imaging.* Bioluminescence imaging was done in the IVIS 100 under 2.5% isoflurane anesthesia, as described previously (20). First, background signals were recorded by imaging before hydrodynamic injections (D-luciferin, 150 mg/kg of body weight, i.p.). Rluc activity was acquired 20 hours after hydrodynamic injections by injection of coelenterazine (1 mg/kg of body weight, i.v.) to serve as a transfection control. Four hours later (generally no residual signal), D-luciferin (150 mg/kg of body weight, i.p.) was given, followed by image acquisition 10 minutes post injection, providing the pretreatment (0 h) activity. Immediately after pretreatment IVIS imaging, groups of mice were treated with Rap (4.5 mg/kg in DMSO, i.p.; $n = 6$ for FRB-VP16 pair; $n = 2$ for mtFRB-VP16 pair) or vehicle only (DMSO; $n = 2$). At the indicated times after treatment with Rap (6, 15, 24, 48, and 72 h), mice were again injected with D-luciferin (i.p.) and imaged 10 minutes later (IVIS 100). Because of the highly inducible nature of the photon output, images 24 hours after Rap treatment were obtained with different exposure times (1-10 s) compared with those at later time points in the experiment (exposure time, 5 min) to avoid saturation of the charge-coupled device camera. Photon flux (photons per second) was quantified on images by contour-based regions of interests, in which the edge of the region of interest was defined as 40% of peak values and analyzed with Living Image 2.6 (Caliper) and IGOR (WaveMetrics) image analysis software. Data represent the mean ± SE or range in each group imaged over the course of the experiment and are expressed relative to the pretreatment bioluminescence of the same mouse (photon flux, fold-initial).

Western blotting

HeLa/*Gal4→Fluc* cells (3×10^6 per 10-cm dish) were transfected with the indicated pairs of plasmids (3 μg DNA each), followed by bioluminescence imaging 48 hours after transfection. After a PBS wash, whole-cell lysates were prepared in 10 mmol/L Tris (pH 8.5) and 1% SDS, and freshly combined with sodium orthovanadate (1 mmol/L) and protease inhibitor cocktail (1:100; Sigma-Aldrich). Protein concentration was determined by bicinchoninic acid assay (Pierce). Proteins (50 μg) were fractionated by SDS-PAGE and immunoblotted with primary antibodies for VP16 (1:100; Abcam) and G4BD (1:500; Santa Cruz Biotechnology). Immunoblots of G4BD were stripped and reprobed with anti-actin antibody (1:2,000; Sigma-Aldrich). Bound primary antibodies were visualized with appropriate horseradish peroxidase–conjugated secondary antibodies (1:1,000) with the use of enhanced chemiluminescence (Amersham Pharmacia, GE Healthcare).

A cohort of mice was subjected to hydrodynamic injections and bioluminescence imaging before and at the indicated times after treatment with Rap or vehicle (6, 24, and 72 h) as above. Immediately after imaging, livers were harvested and ~3 g of tissue were placed into 1 mL of lysis buffer [50 mmol/L Tris (pH 8), 100 mmol/L NaCl, 5 mmol/L EDTA, 0.5% P40) freshly combined with sodium orthovanadate (1 mmol/L), protease and phosphatase inhibitor cocktail (1:100; Sigma-Aldrich), and phenylmethylsulfonyl fluoride (2 mmol/L), and homogenized at 4°C with the use of a homogenizer (PT3000, Brinkmann). Samples were then centrifuged twice for 10 minutes at 14,000 *g* to remove cell debris. Protein concentration measurement and Western blotting were done

Published OnlineFirst September 21, 2010; DOI: 10.1158/1535-7163.MCT-10-0265

as described above. Proteins (500 μg) were fractionated by SDS-PAGE and immunoblotted with primary antibodies for phosphorylated p70S6 kinase (p70S6K; S371; 1:1,000; Cell Signaling Technology) and actin. Immunoblots were stripped and reprobed with anti-p70S6K antibodies (1:1,000; Cell Signaling Technology).

Statistics

Curve-fitting, EC_{50}, K_d, and K_i values were determined with Prism software (GraphPad). All data are presented as mean ± SE or range.

Results

In vitro studies

Concentration response of Rap-induced protein-protein interactions and competitive inhibition by FK506. In HeLa/*Gal4→Fluc* cells coexpressing the FRB-VP16 and G4BD-FKBP chimera protein pairs, Rap increased bioluminescence signals in a concentration-dependent manner up to 3 nmol/L. Maximum induction was 628-fold over baseline 6 hours after addition of 3 nmol/L of drug (Fig. 2). Curve fitting of the data revealed an EC_{50} of 1.2 ± 0.02 nmol/L with an apparent K_d of 2.3 ± 1.1 nmol/L ($n = 3$). Under these conditions, reporter signals declined at concentrations >3 nmol/L (Supplementary Fig. S1). Addition of FK506, a competitive inhibitor of Rap binding to FKBP, inhibited Rap-induced luciferase activity in the presence of 1 nmol/L of Rap with a K_i of 17.1 nmol/L, derived with the use of the Cheng-Prusoff equation (ref. 28; $n = 3$; Fig. 3).

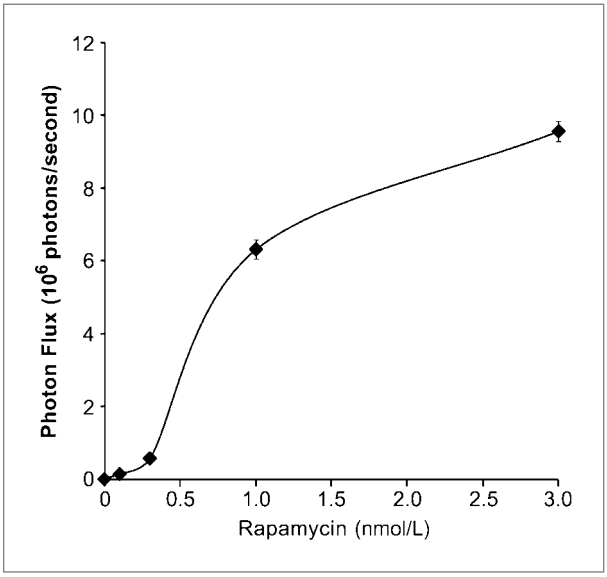

Figure 2. Concentration-dependent Rap-induced FRB/FKBP interactions. HeLa/*Gal4→Fluc* reporter cells were cotransfected with plasmid pairs expressing FRB-VP16 and G4BP-FKBP and then treated with various concentrations of Rap for 6 hours. Bioluminescence signals increased in a concentration-dependent manner up to 3 nmol/L (K_d = 2.3 ± 1.1 nmol/L). Data, mean photon flux ± SE (when larger than symbol) of triplicate wells.

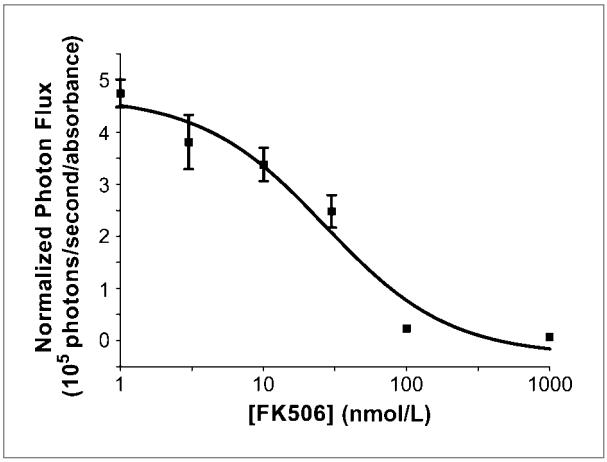

Figure 3. Competitive inhibition by FK506. HeLa/*Gal4→Fluc* cells coexpressing FRB-VP16 and G4BD-FKBP were treated with Rap at the EC_{50} (1 nmol/L) as well as the indicated concentrations of FK506 for 6 hours. The K_i of FK506-mediated inhibition of Rap-induced protein association was determined with the Cheng-Prusoff equation (K_i = 17.1 nmol/L). Data, mean photon flux normalized to cell mass ± SE (when larger than symbol) of triplicate wells.

Abrogation of FRB and FKBP12 association by mutant FRB (S2035I). HeLa/*Gal4→Fluc* cells transiently transfected with plasmids expressing FRB-VP16 together with G4BD-FKBP and treated with 1 nmol/L Rap produced 100-fold greater bioluminescence signals than vehicle-treated cells (Fig. 4A). In comparison, the coexpression of mtFRB-VP16 and G4BD-FKBP produced no significant change in bioluminescence activity after treatment with 1 nmol/L Rap ($P \gg 0.05$). Western blots of whole-cell lysates showed similar expression levels of both FRB-VP16 and mtFRB-VP16 proteins, as well as G4BD-FKBP proteins under each condition (Fig. 4B). Whereas quantitative analysis showed a 35% decrease in protein levels for mtFRB compared with wild-type, the complete disruption of the Rap-induced bioluminescence signal with mtFRB-VP16 was most consistent with abrogation of Rap binding by mutation of ser^{2035} within FRB (29) rather than loss of protein.

In vivo studies

Rap-induced bioluminescence in Gal4→Fluc transgenic reporter mice. To show that Rap-induced transactivation of the reporter gene could be imaged in living animals, we did somatic gene transfer by giving plasmid pairs expressing wild-type FRB-VP16 and G4BD-FKBP, or mtFRB-VP16 and G4BD-FKBP along with Rluc through hydrodynamic injection into *Gal4→Fluc* reporter mice. We obtained images of mice before hydrodynamic injection, before Rap or vehicle treatment (0 h), and at the indicated times after treatment (6 to 72 h). Photon flux from *Rluc* expression in the liver, obtained 4 hours before Rap exposure (−4 h), showed comparable transfection efficiency of hydrodynamic injection among all three groups (Fig. 5A, left). After Rap treatment, photon flux arising

Published OnlineFirst September 21, 2010; DOI: 10.1158/1535-7163.MCT-10-0265

from *Fluc* expression in the livers of mice receiving FRB-VP16 and G4BD-FKBP reached maximal levels at 24 hours and persisted for 3 days, at which point the signal declined back to almost pretreatment levels (Fig. 5A, top). The signal 24 hours after Rap treatment was almost 600-fold higher than the pretreatment baseline (Fig. 5B), achieving photon flux values of $4.6 \times 10^8 \pm 1.1 \times 10^8$ photons per second.

As a control, mice were injected with the FRB-VP16 and G4BD-FKBP pair, treated with vehicle, and imaged over the same time course as described above. Vehicle had no effect on transactivation of the reporter gene (Fig. 5A, middle). Furthermore, mice expressing the mtFRB-VP16 and G4BD-FKBP pair showed no detectable signal induction in response to Rap treatment over the entire time course of the experiment (Fig. 5A, bottom; Fig. 5B).

Attenuation of mTOR signaling after Rap treatment in transgenic reporter mice. To independently validate functional mTOR activity in reporter mice in response to Rap treatment, we monitored phosphorylated p70S6K (S371), a downstream effector of mTOR, by Western analysis in another cohort of reporter mice subjected to hydrodynamic injection and bioluminescence imaging. Immediately after imaging, liver samples were harvested at the indicated times post Rap or vehicle treatment. Bioluminescence imaging results were similar to those shown in Fig. 5 (data not shown). When normalized to total p70S6K and baseline levels before Rap treatment, phosphorylated p70S6K (S371) was attenuated at 6 (0.33) and 24 hours (0.21) post Rap exposure, and returned toward baseline at 72 hours (0.63; Fig. 6A, top). Total p70S6K remained unperturbed (Fig. 6A, middle). In contrast, there was no substantial difference in phosphorylated p70S6K (S371) in response to vehicle treatment (Fig. 6B).

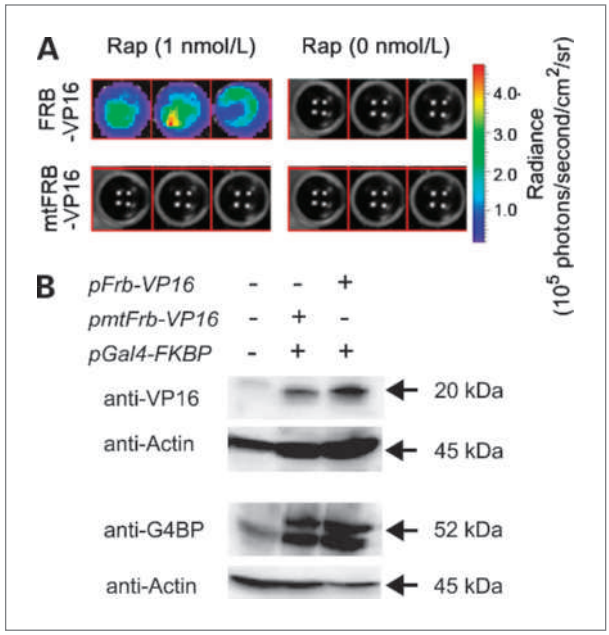

Figure 4. Disruption of Rap-induced protein associations by mutant FRB (mtFRB) *in cellulo*. Compared with untreated cells, HeLa/*Gal4→Fluc* cells transiently expressing FRB-VP16 and G4BD-FKBP produced 100-fold greater bioluminescence signals after treatment with 1 nmol/L Rap for 6 hours (A, top). In contrast, cells transfected with the plasmid pair expressing mtFRB produced no significant signal change after Rap treatment ($P \gg 0.05$; A, bottom). Western blot analysis (B) showed comparable expression of FRB-VP16, mtFRB-VP16, as well as G4BP-FKBP from cotransfected HeLa/*Gal4→Fluc* cells treated with Rap (1 nmol/L) for 6 hours.

Discussion

Rapamycin, or Sirolimus, is approved as an antirejection agent post organ transplantation and confers immunosuppressant properties through suppression of interleukin 2–induced T-cell proliferation and activation (30). Rapamycin-coated stents are also Food and Drug Administration–approved to reduce restenosis after coronary artery intervention through inhibition of vascular smooth cells (31, 32). Because of the versatile therapeutic potential of rapamycin associated with the mTOR signaling pathway as well as immunophilin function, various rapamycin analogues with modified and improved pharmacokinetic properties have been developed as effective therapeutics for organ transplantation, cancer, restenosis, and neurodegenerative disorders (10). Temsirolimus and everolimus are Food and Drug Administration–approved rapamycin analogues for the treatment of advanced renal cell carcinoma through disruption of mTOR signaling, and subsequent suppression of protein translation, cell cycle progression, and angiogenesis (7, 33, 34). Recently, numerous nonimmunosuppressive rapamycin analogues have been developed as novel candidate therapeutics for the treatment of neurodegenerative diseases or stroke after the discovery of potent rapamycin-mediated neuroprotective properties for this class of compounds (35, 36). In addition to mTOR or immunophilin-related signaling pathways, rapamycin analogues also provide unique opportunities to regulate protein function through conditional control of protein stability, localization, and protein-protein interactions *in vivo* (37).

In terms of pharmacodynamic monitoring of rapamycin or its analogues, current strategies use biomarkers derived from either blood, skin, or tumor samples of patients (38, 39). Real-time reverse transcriptase-PCR, Western blot, or immunohistochemical analysis for biomarkers, such as cytokines (interleukin 2, 4 or 10), or downstream targets of mTOR, such as eukaryotic initiation factor 4E–binding protein 1 or p70S6K, have been reported (5, 40, 41). However, a sensitive approach to quantitatively interrogate the pharmacodynamics of Rap or its analogues in mouse models over time is lacking.

In vivo imaging, compared with conventional methods to monitor pharmacodynamics, permits the evaluation of drug effects on the target with quantitative, spatiotemporal resolution after various dosages and at any given time of interest (17, 18). Such a strategy will

Published OnlineFirst September 21, 2010; DOI: 10.1158/1535-7163.MCT-10-0265

efficiently verify the effects of drugs of interest in living organisms, such as reporter animals, without the requirement of high-quality antibodies and laborious sample processing. Most importantly, it enables noninvasive and longitudinal observation of target engagement and may help minimize the costs and time of pharmaceutical development.

The results of the present study show the application of bioluminescence imaging to monitor the pharmacodynamics of Rap in a continuous and noninvasive manner with the use of transgenic mice that incorporate a genetically encoded two-hybrid reporter strategy. In effect, the system allows a molecular-specific pharmacodynamic readout of Rap in living mice. The data reported herein show that Rap induced protein-protein interactionsin a concentration-dependent and FK506-competitive manner. The K_d value derived from the transcriptional readout (2.3 ± 1.1 nmol/L) compared favorably with previously reported values determined by luciferase and colorimetric complementation systems *in cellulo* (42, 43). Accordingly, in our system, FK506, a competitive inhibitor of Rap, diminished Rap-induced bioluminescence signals with a K_i of 17.1 nmol/L, which is also comparable with the K_i of

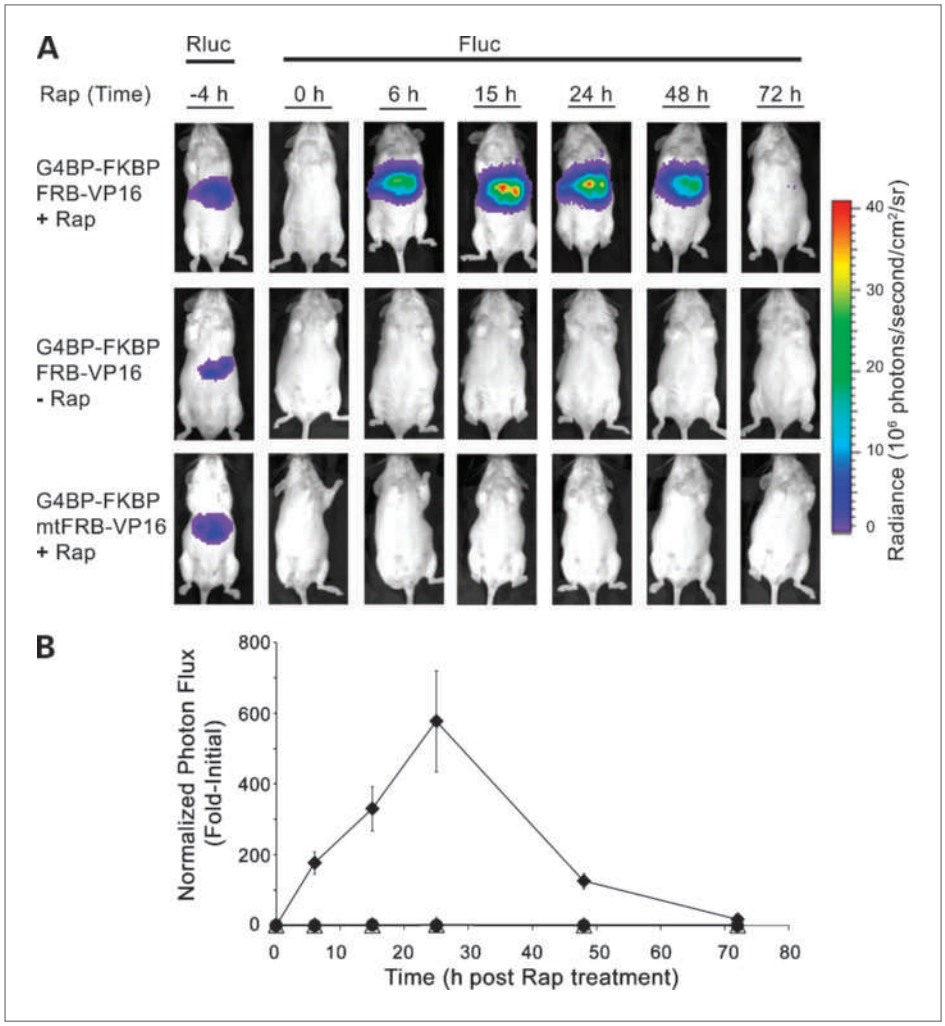

Figure 5. Pharmacodynamic analysis of Rap by bioluminescence imaging *in vivo*. Somatic gene transfer was done by hydrodynamic injection of plasmid pairs expressing FRB-VP16 and G4BD-FKBP, or mtFRB-VP16 and G4BD-FKBP (along with Rluc as a transfection control) into *Gal4→Fluc* transgenic reporter mice. Mice were imaged before and after treatment with Rap (4.5 mg/kg, i.p.) or vehicle at the indicated times. A, transfection efficiency was similar between the groups as indicated by Rluc signals (left, representative images). Transgenic reporter mice receiving wild-type plasmid pairs (top, representative of $n = 6$) produced peak Fluc signals 24 hours after Rap treatment ($4.6 \times 10^8 \pm 1.1 \times 10^8$ photons per second) and returned to baseline within 72 hours. Mice treated with vehicle showed no Fluc response (middle, representative of $n = 2$); mice receiving the mutant plasmid pair and treated with Rap also showed no Fluc response (bottom, representative of $n = 2$). B, Rap-induced normalized photon flux (Fluc; fold-initial) as a function of time. Wild-type FRB-VP16/G4BD-FKBP–induced signal increased 600-fold over the pretreatment baseline at 24 hours post Rap treatment. Data, means ± SE or range (when larger than symbol); diamond, FRB-VP16 and G4BP-FKBP with Rap; triangle, FRB-VP16 and G4BP-FKBP with vehicle; circle, mtFRB-VP16 and G4BP-FKBP with Rap.

Published OnlineFirst September 21, 2010; DOI: 10.1158/1535-7163.MCT-10-0265

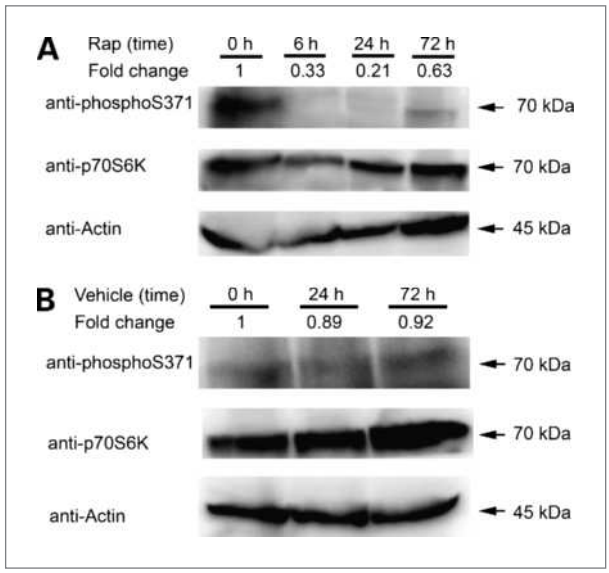

Figure 6. Suppression of p70S6K phosphorylation by Rap treatment in reporter mice. Somatic gene transfer by hydrodynamic injection and subsequent bioluminescence imaging of *Gal4→Fluc* transgenic reporter mice were followed by harvest of liver samples before and at the indicated times post Rap or vehicle exposure. A, Western blot analysis showed attenuation of phosphorylated p70S6K (S371) at 6 and 24 hours post Rap treatment and recovery toward baseline at 72 hours. The fold-change of phosphorylated p70S6K (S371) was normalized to the corresponding total p70S6K protein. B, phosphorylated p70S6K (S371) was relatively unaffected by vehicle treatment.

FK506 in other reported *in vitro* systems (42, 44). Note that our *in vivo* reporter system showed a high level of signal induction (600-fold) 24 hours after treatment with Rap. In contrast, expression of mutant FRB (mtFRB S2035I), which abrogates binding to Rap, did not activate the reporter system *in cellulo* or *in vivo*. The slightly decreased mtFRB protein expression level observed in cells, compared with that of wtFRB, could have resulted from the destabilized quality of mtFRB when not bound to Rap (3).

One arm of mTOR signaling controls translation through activation of p70S6K and inhibition of eukaryotic initiation factor 4E–binding protein 1 (41, 45, 46). Therefore, we used antibodies specific for S371 phosphorylation of p70S6K, a Rap-sensitive phosphorylation site critical for kinase activity, as an independent readout of mTOR activity (47, 48). As anticipated, suppression of p70S6K phosphorylation induced by Rap treatment correlated temporally with induction of bioluminescence signals, peaking at 24 hours post Rap exposure *in vivo*, further validating the reporter strategy.

Note that reporter signals *in cellulo* produced by Rap-induced protein association plateaued in the presence of ~3 nmol/L Rap and began to decrease as the concentration increased (Supplementary Fig. S1). This may have been due to the mechanism of action of Rap, which resulted in inhibition of mTOR signaling, thereby enhancing autophagy, repressing ribosomal protein synthesis, and inhibiting translation over the time frame of these experiments (8, 9, 49). The transcriptional readout strategy may be sensitive to this Rap-induced activity over time and therefore fail to fully engage reporter machinery after exposure to high concentrations of Rap for 6 hours and longer. This stands in contrast to luciferase protein fragment complementation strategies, in which readouts occurred within minutes, results were not dependent on new protein synthesis, and suppression of signals at high concentrations of Rap were not observed (42).

In vivo imaging is a field of ongoing and active research in which genetically encoded reporters in conjunction with optical imaging, including bioluminescence and fluorescence imaging, can add significant value to the drug development process due to their efficiency, low cost, and sensitivity (17, 18). An effective reporter animal model can serve as a useful tool to monitor the effects of candidate drugs and bridge the preclinical studies to successful clinical translation. In the current study, our highly inducible *Gal4→Fluc* transgenic reporter mice proved to be amenable to verifying the pharmacodynamic effects of Rap on the basis of an *in vivo* mouse two-hybrid system. Our mouse two-hybrid transgenic model seems to have inherent high sensitivity while engaging the platform in an appropriate mammalian context. In contrast, conventional yeast two-hybrid assays are often criticized for generating high rates of false positive outputs (50), perhaps related to the study of protein-protein interactions of human gene products within the context of yeast, which do not necessarily reproduce the relevant microenvironment, physiologic context, and subcellular localization required for high-fidelity results (51). The mouse two-hybrid system allows future high-throughput assays based on monitoring changes in protein-protein interactions in response to novel pharmaceutical reagents in an environment better recapitulating human physiology. Furthermore, reporter systems with transcriptional amplification can enhance reporter gene expression from relatively weak promoters, such as the *Gal4* promoter in our system (52, 53). Compared with other existing modalities to address protein-protein interactions, such as bioluminescence resonance energy transfer systems and split reporter protein complementation, this signal amplification character secondary to transcriptional cascades will be valuable in systems in which the signal output is low. On the other hand, a major caveat is the sacrifice in temporal resolution with transcriptional reporter strategies, both in terms of on rates as well as off rates, compared with post-translational strategies (54).

In conclusion, we showed the feasibility of a mouse two-hybrid platform with the use of a highly inducible *Gal4→Fluc* reporter mouse to monitor conditional protein-protein interactions at the level of transcriptional readouts with the use of bioluminescence imaging. This reporter model may better reflect physiologic conditions in which protein-protein interactions are under intricate layers of control as well as provide a more

Published OnlineFirst September 21, 2010; DOI: 10.1158/1535-7163.MCT-10-0265

sensitive assessment inherent to the broad dynamic range of this approach (20). This strategy may facilitate imaging studies of protein interactions, signaling cascades, and drug development within the physiologic context of living animals.

Disclosure of Potential Conflicts of Interest

No potential conflicts of interest were disclosed.

Grant Support

NIH grant P50 CA94056 and a Fellowship from the Cancer Biology Pathway training program through the Alvin J. Siteman Cancer Center at Barnes-Jewish Hospital–Washington University School of Medicine (M-H. Pan).

The costs of publication of this article were defrayed in part by the payment of page charges. This article must therefore be hereby marked *advertisement* in accordance with 18 U.S.C. Section 1734 solely to indicate this fact.

Received 03/16/2010; revised 07/15/2010; accepted 07/29/2010; published OnlineFirst 09/21/2010.

References

1. Abraham RT, Eng CH. Mammalian target of rapamycin as a therapeutic target in oncology. Expert Opin Ther Targets 2008;12:209–22.
2. Choi J, Chen J, Schreiber SL, Clardy J. Structure of the FKBP12-rapamycin complex interacting with the binding domain of human FRAP. Science 1996;273:239–42.
3. Edwards SR, Wandless TJ. The rapamycin-binding domain of the protein kinase mammalian target of rapamycin is a destabilizing domain. J Biol Chem 2007;282:13395–401.
4. Groth CG, Backman L, Morales JM, et al. Sirolimus European Renal Transplant Study Group. Sirolimus (rapamycin)-based therapy in human renal transplantation: similar efficacy and different toxicity compared with cyclosporine. Transplantation 1999;67:1036–42.
5. Sessa C, Tosi D, Vigano L, et al. Phase Ib study of weekly mammalian target of rapamycin inhibitor ridaforolimus (AP23573; MK-8669) with weekly paclitaxel. Ann Oncol 2010;21:1315–22.
6. Galanis E, Buckner JC, Maurer MJ, et al. Phase II trial of temsirolimus (CCI-779) in recurrent glioblastoma multiforme: a North Central Cancer Treatment Group study. J Clin Oncol 2005;23:5294–304.
7. Hudes G, Carducci M, Tomczak P, et al. Temsirolimus, interferon α, or both for advanced renal-cell carcinoma. N Engl J Med 2007;356:2271–81.
8. Kamada Y, Funakoshi T, Shintani T, Nagano K, Ohsumi M, Ohsumi Y. Tor-mediated induction of autophagy via an Apg1 protein kinase complex. J Cell Biol 2000;150:1507–13.
9. Zaragoza D, Ghavidel A, Heitman J, Schultz MC. Rapamycin induces the G0 program of transcriptional repression in yeast by interfering with the TOR signaling pathway. Mol Cell Biol 1998;18:4463–70.
10. Graziani EI. Recent advances in the chemistry, biosynthesis and pharmacology of rapamycin analogs. Nat Prod Rep 2009;26:602–9.
11. Hedley DW, Chow S, Goolsby C, Shankey TV. Pharmacodynamic monitoring of molecular-targeted agents in the peripheral blood of leukemia patients using flow cytometry. Toxicol Pathol 2008;36:133–9.
12. Liebes L, Potmesil M, Kim T, et al. Pharmacodynamics of topoisomerase I inhibition: western blot determination of topoisomerase I and cleavable complex in patients with upper gastrointestinal malignancies treated with topotecan. Clin Cancer Res 1998;4:545–57.
13. Baselga J, Albanell J, Ruiz A, et al. Phase II and tumor pharmacodynamic study of gefitinib in patients with advanced breast cancer. J Clin Oncol 2005;23:5323–33.
14. Sarker D, Workman P. Pharmacodynamic biomarkers for molecular cancer therapeutics. Adv Cancer Res 2007;96:213–68.
15. Chautard E, Thierry-Mieg N, Ricard-Blum S. Interaction networks: from protein functions to drug discovery. A review. Pathol Biol (Paris) 2009;57:324–33.
16. Ferrer-Alcon M, Arteta D, Guerrero MJ, Fernandez-Orth D, Simon L, Martinez A. The use of gene array technology and proteomics in the search of new targets of diseases for therapeutics. Toxicol Lett 2009;186:45–51.
17. Gross S, Piwnica-Worms D. Molecular imaging strategies for drug discovery and development. Curr Opin Chem Biol 2006;10:334–42.
18. Stell A, Belcredito S, Ramachandran B, et al. Multimodality imaging: novel pharmacological applications of reporter systems. Q J Nucl Med Mol Imaging 2007;51:127–38.
19. US Code of Federal Regulations; vol 21, pp. 500–60.
20. Pichler A, Prior JL, Luker GD, Piwnica-Worms D. Generation of a highly inducible *Gal4→Fluc* universal reporter mouse for *in vivo* bioluminescence imaging. Proc Natl Acad Sci U S A 2008;105:15932–7.
21. Berman HM, Westbrook J, Feng Z, et al. The Protein Data Bank. Nucleic Acids Res 2000;28:235–42.
22. Odagaki Y, Clardy J. Structural basis for peptidomimicry by the effector element of rapamycin. J Am Chem Soc 1997;119:10253.
23. Jonker HR, Wechselberger RW, Boelens R, Folkers GE, Kaptein R. Structural properties of the promiscuous VP16 activation domain. Biochemistry 2005;44:827–39.
24. Wilson KP, Yamashita MM, Sintchak MD, et al. Comparative X-ray structures of the major binding protein for the immunosuppressant FK506 (tacrolimus) in unliganded form and in complex with FK506 and rapamycin. Acta Crystallogr D Biol Crystallogr 1995;51:511–21.
25. Hong M, Fitzgerald MX, Harper S, Luo C, Speicher DW, Marmorstein R. Structural basis for dimerization in DNA recognition by Gal4. Structure 2008;16:1019–26.
26. Bayle JH, Grimley JS, Stankunas K, Gestwicki JE, Wandless TJ, Crabtree GR. Rapamycin analogs with differential binding specificity permit orthogonal control of protein activity. Chem Biol 2006;13:99–107.
27. Gross S, Piwnica-Worms D. Real-time imaging of ligand-induced IKK activation in intact cells and in living mice. Nat Methods 2005;2:607–14.
28. Cheng Y, Prusoff W. Relationship between inhibition constant (ki) and the concentration of the inhibitor which causes 50% inhibition (I50) of an enzymatic reaction. Biochem Pharmacol 1973;22:3099–108.
29. Chen J, Zheng XF, Brown EJ, Schreiber SL. Identification of an 11-kDa FKBP12-rapamycin-binding domain within the 289-kDa FKBP12-rapamycin-associated protein and characterization of a critical serine residue. Proc Natl Acad Sci U S A 1995;92:4947–51.
30. Lai JH, Tan TH. CD28 signaling causes a sustained down-regulation of I κ B α which can be prevented by the immunosuppressant rapamycin. J Biol Chem 1994;269:30077–80.
31. Serruys PW, Kutryk MJ, Ong AT. Coronary-artery stents. N Engl J Med 2006;354:483–95.
32. Poon M, Marx SO, Gallo R, Badimon JJ, Taubman MB, Marks AR. Rapamycin inhibits vascular smooth muscle cell migration. J Clin Invest 1996;98:2277–83.
33. Motzer RJ, Escudier B, Oudard S, et al. Efficacy of everolimus in advanced renal cell carcinoma: a double-blind, randomised, placebo-controlled phase III trial. Lancet 2008;372:449–56.
34. Atkins MB, Yasothan U, Kirkpatrick P. Everolimus. Nat Rev Drug Discov 2009;8:535–6.
35. Lyons WE, George EB, Dawson TM, Steiner JP, Snyder SH. Immunosuppressant FK506 promotes neurite outgrowth in cultures of PC12 cells and sensory ganglia. Proc Natl Acad Sci U S A 1994;91:3191–5.
36. Ruan B, Pong K, Jow F, et al. Binding of rapamycin analogs to calcium channels and FKBP52 contributes to their neuroprotective activities. Proc Natl Acad Sci U S A 2008;105:33–8.
37. Banaszynski LA, Sellmyer MA, Contag CH, Wandless TJ, Thorne SH. Chemical control of protein stability and function in living mice. Nat Med 2008;14:1123–7.

Published OnlineFirst September 21, 2010; DOI: 10.1158/1535-7163.MCT-10-0265

38. Jimeno A, Rudek MA, Kulesza P, et al. Pharmacodynamic-guided modified continuous reassessment method-based, dose-finding study of rapamycin in adult patients with solid tumors. J Clin Oncol 2008;26:4172–9.

39. Johnson BE, Jackman D, Janne PA. Rationale for a phase I trial of erlotinib and the mammalian target of rapamycin inhibitor everolimus (RAD001) for patients with relapsed non small cell lung cancer. Clin Cancer Res 2007;13:s4628–31.

40. Muller-Steinhardt M, Wortmeier K, Fricke L, Ebel B, Hartel C. The pharmacodynamic effect of sirolimus: individual variation of cytokine mRNA expression profiles in human whole blood samples. Immunobiology 2009;214:17–26.

41. Tanaka C, O'Reilly T, Kovarik JM, et al. Identifying optimal biologic doses of everolimus (RAD001) in patients with cancer based on the modeling of preclinical and clinical pharmacokinetic and pharmacodynamic data. J Clin Oncol 2008;26:1596–602.

42. Luker KE, Smith MC, Luker GD, Gammon ST, Piwnica-Worms H, Piwnica-Worms D. Kinetics of regulated protein-protein interactions revealed with firefly luciferase complementation imaging in cells and living animals. Proc Natl Acad Sci U S A 2004;101:12288–93.

43. Galarneau A, Primeau M, Trudeau L-E, Michnick S. b-Lactamase protein fragment complementation assays as *in vivo* and *in vitro* sensors of protein-protein interactions. Nat Biotechnol 2002;20:619–22.

44. Remy I, Michnick S. Clonal selection and *in vivo* quantitation of protein interactions with protein-fragment complementation assays. Proc Natl Acad Sci U S A 1999;96:5394–9.

45. Shama S, Meyuhas O. The translational cis-regulatory element of mammalian ribosomal protein mRNAs is recognized by the plant translational apparatus. Eur J Biochem 1996;236:383–8.

46. Hara K, Yonezawa K, Weng QP, Kozlowski MT, Belham C, Avruch J. Amino acid sufficiency and mTOR regulate p70 S6 kinase and eIF-4E BP1 through a common effector mechanism. J Biol Chem 1998;273:14484–94.

47. Moser BA, Dennis PB, Pullen N, et al. Dual requirement for a newly identified phosphorylation site in p70s6k. Mol Cell Biol 1997;17:5648–55.

48. Turck F, Kozma SC, Thomas G, Nagy F. A heat-sensitive *Arabidopsis thaliana* kinase substitutes for human p70s6k function *in vivo*. Mol Cell Biol 1998;18:2038–44.

49. Cruz MC, Goldstein AL, Blankenship J, et al. Rapamycin and less immunosuppressive analogs are toxic to *Candida albicans* and *Cryptococcus neoformans* via FKBP12-dependent inhibition of TOR. Antimicrob Agents Chemother 2001;45:3162–70.

50. Vidalain PO, Boxem M, Ge H, Li S, Vidal M. Increasing specificity in high-throughput yeast two-hybrid experiments. Methods 2004;32:363–70.

51. Figeys D. Mapping the human protein interactome. Cell Res 2008;18:716–24.

52. Iyer M, Wu L, Carey M, Wang Y, Smallwood A, Gambhir S. Two-step transcriptional amplification as a method for imaging reporter gene expression using weak promoters. Proc Natl Acad Sci U S A 2001;98:14595–600.

53. Griggs DW, Johnston M. Promoter elements determining weak expression of the GAL4 regulatory gene of *Saccharomyces cerevisiae*. Mol Cell Biol 1993;13:4999–5009.

54. Villalobos V, Naik S, Piwnica-Worms D. Current state of imaging protein-protein interactions *in vivo* with genetically encoded reporters. Annu Rev Biomed Eng 2007;9:321–49.

Published OnlineFirst September 21, 2010; DOI: 10.1158/1535-7163.MCT-10-0265

Molecular Cancer Therapeutics

Monitoring Molecular-Specific Pharmacodynamics of Rapamycin *In vivo* with Inducible *Gal4→Fluc* Transgenic Reporter Mice

Mei-Hsiu Pan, Jeffrey Lin, Julie L. Prior, et al.

Mol Cancer Ther Published OnlineFirst September 21, 2010.